

Modelling of optical absorption of silver NP's produced by UV radiation embedded in mesostructured silica films

Guadalupe Valverde-Aguilar · Jorge A. García-Macedo ·

Víctor M. Rentería-Tapia · Raúl W. Gómez ·

Manuel Quintana-García

Received: 27 April 2010/Accepted: 13 May 2011

© Springer Science+Business Media B.V. 2011

Abstract Hexagonal mesostructured films containing silver ions were obtained by sol–gel method. Brij 58 was used to produce channels into the film, which house these ions. The films were exposure to UV radiation to produced silver metallic nanoparticles. The presence of the metallic nanoparticles was determined by infrared spectroscopy and optical absorption. Besides, these nanoparticles and core–shell structures of silver–silver oxide nanoparticles were identified by high-resolution transmission electronic microscopy. From these measurements, the

obtained size range for silver nanoparticles was 6.1 nm. The absorption spectrum located at 440 nm was modelled and well fitted with the Gans theory considering refractive index higher than the one coming from host matrix. This index is explained because the silver oxide shell modifies the local surrounding medium of the metallic nanoparticles.

Keywords Gans theory · Core–shell · Sol–gel · Silver nanoparticles · Block copolymers · Refractive index · Modeling and simulation · Thin film

G. Valverde-Aguilar (✉)

CICATA Unidad Legaria, IPN, Legaria 694, Col Irrigación, Miguel Hidalgo, C. P. 11500 Ciudad de México, DF, México
e-mail: valverdeag@gmail.com

J. A. García-Macedo

Departamento de Estado Sólido, Instituto de Física, Universidad Nacional Autónoma de México, C. P. 04510 México, DF, México
e-mail: gamaj@fisica.unam.mx

V. M. Rentería-Tapia

Departamento de Ciencias Naturales y Exactas, Universidad de Guadalajara, Centro Universitario de los Valles, C. P. 46600 Ameca, JAL, México
e-mail: victor.renteria@profesores.valles.udg.mx

R. W. Gómez · M. Quintana-García

Facultad de Ciencias, Universidad Nacional Autónoma de México, Av. Universidad 3000, Copilco el Bajo, Coyoacán, 04510 México, DF, México
e-mail: rgomez@servidor.unam.mx

Introduction

Metallic nanoparticles (NP's) embedded in amorphous SiO₂ glasses (dielectric matrix) have attracted a great deal of attention over past decade due to their interesting optical properties and their technological applications in photo electrodes for solar cells (Kozuka 1997), optical switches (Weiping et al. 1996), electronic and magnetic devices, catalysis or sensors (Masumoto and Kawamura 1993; Sun et al. 2003; Compagnini et al. 2002; Naoi et al. 2004). These properties depend on the size, shape and dielectric environment surrounding the NP's (Naoi et al. 2004). The metallic NP's may be incorporated as individual primary particles or as agglomerated particles (secondary particles), and the primary or secondary particles can be arranged randomly or in an ordered or oriented state, depending on the method

of nanocomposite preparation and processing. In order to avoid agglomeration, the NP's are frequently synthesised *in situ* or surface modified agents can be applied, where a spherical inorganic core is preferentially surrounded by a shell composed of organic molecules (core–shell particles) (Caseri 2006). Other mechanism to produced metallic NP's is in the presence of surfactants (Liz-Marzán and Lado-Touriño 1996), which reduces the silver ions to the neutral state through oxidation of oxyethylene groups to hydroperoxides. Surfactant molecules subsequently adsorb onto the surface of the particles, promoting a steric stabilization (Liz-Marzán and Lado-Touriño 1996). Cubic, hexagonal or lamellar mesostructures can be obtained by controlling the surfactant concentration (Alberius et al. 2002). The dimension of the pore can be controlled using different types of block copolymers (Smarsly et al. 2001).

The metallic NP's exhibit the property of optical absorption originated from a collective oscillation of the conduction electrons when they are excited by light. It is named as surface plasmon resonance. The optical response depends of several factors as the local refractive index (Naou et al. 2004), the dielectric constant of the medium (host matrix and coating), morphology (size and geometry) and state of aggregation of the metallic NP's (Xu and Käll 2002). Any change of these physical features will alter the peak position, intensity or shape of the optical response. Many classical models have been used in order to understand the optical absorption spectra of the metallic NP's (Winkler et al. 1999). The optical absorption can be calculated by the Gans theory, an extended Mie's theory to prolate or oblate particles averaged over all orientations (Link et al. 1999).

In this study, we described the synthesis of long-ordered mesostructured silica films doped with silver nitrate (AgNO_3) under acidic conditions. An ethylene oxide based non-ionic diblock copolymer Brij 58 ($\text{C}_{16}\text{H}_{33}\text{PEO}_{20}$) was added and it plays two important roles: (i) it was used as template for silica polymerization in the synthesis of uniformly distributed silver-ion-containing mesostructured silica films, and (ii) it can be used in the reduction of Ag^+ ions embedded into mesostructured silica matrix to produce silver metallic NP's (Liz-Marzán and Lado-Touriño 1996). This surfactant can stabilize the metallic NP's to avoid their agglomeration into the silica matrix.

The reduction by UV light of Ag^+ ions embedded into mesostructured silica matrix to silver metallic NP's was monitored by UV–Vis absorption spectroscopy. Gans theory including a variable refractive index (Rentería-Tapia and García-Macedo 2005, 2006) was used to fit the experimental absorption spectrum and these results are discussed. They indicate that it is necessary to consider the presence of oxidized metallic NP's in order to have a good fit to the experimental data.

Experimental

Glass substrates were cleaned in boiling acidic solution of sulphuric acid– H_2O_2 (4:1) under stirring for 30 min. They were then placed in deionized water and boiled for 30 min, rinsed three times with deionized water, and stored in deionized water at room temperature. Films were dip-coated on glass substrates ($9 \times 1 \times 1 \text{ cm}^3$) at a rate of 5.3 cm/min. The films were drawn with the equipment described previously that uses hydraulic motion to produce a steady and vibration-free withdrawal of the substrate from the sol (Nishida et al. 1995). Convection-free drying was critical to obtain high optical quality films.

All the used reagents were of LR grade (Aldrich). An initial solution was prepared with AgNO_3 (silver nitrate) dissolved in deionized water and nitric acid in a Nalgene plastic beaker. Then 1 g of methanol, 5.4 g of TMOS (tetramethyl orthosilicate, the silicate precursor) and 4 g of the non-ionic diblock copolymer Brij 58 ($\text{C}_{16}\text{H}_{33}\text{PEO}_{20}$) were added to the solution. This solution was refluxed at 50–70 °C for 20 min to homogenize the mixture. To obtain the SiO_2 thin films doped with silver ions, the final molar ratio of TMOS, methanol, nitric acid, H_2O , $\text{C}_{16}\text{H}_{33}\text{PEO}_{20}$ and AgNO_3 was adjusted to 1:0.9:0.13:6.25:0.1:0.06.

The reduction of Ag^+ ions embedded into mesostructured SiO_2 matrix to silver metallic NP's was obtained by the exposition of the film to UV radiation for 6 h. The film was placed at 3 cm under the UV light emitted by a Mineralight lamp Model UVGL-58. This reduction process was monitored by UV–Vis absorption spectroscopy. UV–Vis absorption spectra were obtained on a Thermo Spectronic Genesys 2 spectrophotometer with an accuracy of ± 1 nm over the wavelength range of 300–900 nm.

IR studies were done using a Bruker Tensor 27 IR spectrometer. Raman spectra were obtained using a triple monochromator equipped with a Princeton Instruments LN-CCD. Data were processed by a PC computer. The 530.9-nm line of a Coherent I-300 Krypton laser at ~ 125 mW was used for excitation. The spectra were collected from a solid sample of Brij 58 powder and mesostructured SiO₂ film with silver NP's.

The structure of the final films was characterized with X-ray diffraction (XRD) patterns. These patterns were recorded on a Bruker AXS D8 Advance diffractometer using Ni-filtered CuK α radiation. A step-scanning mode with a step of 0.02° in the range from 1.5 to 10° in 2θ and an integration time of 2 s was used. Another characterization of the morphology and microstructure was achieved from conventional transmission electron microscopy (TEM) and high-resolution transmission electron microscopy (HRTEM) by means of a JEOL FEG 2010 FasTem electron microscope with 1.9 Å resolution (point to point). For TEM and HRTEM studies, the sample was suspended in ethanol in order to disperse the powders and a drop of the sample was deposited on a lacey carbon copper grid as a TEM support. From the HRTEM micrographs, mean particle size and particle size distribution were calculated too.

Gans theory

For spheroid metallic NP's well separated and which size is $R << \lambda$, where λ is the wavelength of the incident light, the optical properties depend mainly on the axial ratio $\Theta = B/A$ (A is the length of the axis of rotation of the spheroid and B is the shorter transversal axis). On these conditions, the optical absorption can be calculated by the Gans theory, an extended Mie's theory to prolate or oblate particles averaged over all orientations (Bohren and Huffman 1983). According with the Gans theory, a splitting of the surface plasmon is predicted in one longitudinal mode along of the major axis and one transversal mode, perpendicular to the first axis. Assuming that the extinction coefficient is only due to the absorption from silver NP's, the absorption coefficient α can be written as (Bohren and Huffman 1983; Pérez-Juste et al. 2005):

$$\alpha = -(\alpha_1 + \alpha_2) \quad (1)$$

where

$$\alpha_1 = \frac{3\phi\omega n^3}{9cp^2} \left\{ \frac{\varepsilon_2(\omega)}{[\varepsilon_1(\omega) + n^2(1/p' - 1)]^2 + \varepsilon_2(\omega)^2} \right\} \quad (2)$$

$$\alpha_2 = \frac{3\phi\omega n^3}{9cp''^2} \left\{ \frac{2\varepsilon_2(\omega)}{[\varepsilon_1(\omega) + n^2(1/p'' - 1)]^2 + \varepsilon_2(\omega)^2} \right\} \quad (3)$$

Specifically, for prolate NP's we have that:

$$p' = \frac{1-e^2}{e^2} \left\{ \frac{1}{2e} \ln \frac{1+e}{1-e} - 1 \right\} \quad (4)$$

$$p'' = \frac{1-p'}{2} \quad (5)$$

$$e = \sqrt{1 + \left(\frac{B}{A} \right)^2} \quad (6)$$

α_1 and α_2 are the components of the absorption coefficient parallel and perpendicular to the longer principal axis of the particle, respectively, ϕ is the volume fraction, c is the light velocity, n is the local refractive index of the medium surrounding the silver NP's, $\varepsilon_1(\omega)$ and $\varepsilon_2(\omega)$ are the real and imaginary part of the dielectric constant of silver in bulk, respectively, The parameters p' and p'' are the depolarization factors for the three axes A , B , C , of the prolate shape with $A > B = C$. The ratio B/A is the axial ratio (Θ).

Moreover, the dielectric constant of the metal bulk must be modified to take into account the decreasing of the electron mean free path in the small particles. This effect will produce an increment in the predicted half-width of the absorption band. The complex dielectric constant correction due to the dependence on the frequency ω and particle size R from the spherical NP's is given as (Rentería-Tapia and García-Macedo 2005)

$$\varepsilon_1(\omega, R) = \varepsilon_1(\omega) \quad (7)$$

$$\varepsilon_2(\omega, R) = \varepsilon_2(\omega) + \eta \frac{\omega_p^2}{\omega^3} \left(\frac{V_f}{R} \right) \quad (8)$$

where $R = 1/2(ABC)^{1/3}$, ω_p is the plasmon frequency and V_f is the Fermi velocity of the conduction electrons. The η parameter is related to the scattering rate of the free electrons against other electrons, the particle surface, phonons, defects and so on (Rentería-Tapia and García-Macedo 2005). Using the

Eqs. 1–8, we can obtain the calculated absorption spectra of silver NP's in 2D-hexagonal mesostructured sol-gel thin films. Thus, the Gans theory can provide information with regards to the size and shape of the metallic NP's as well as of the local refractive index of the medium surrounding the silver NP's.

Results and discussion

IR analysis

Figure 1 shows the IR spectrum from AgNO_3 powder prepared as KBr pellet was measured by transmission and diffuse reflectance. This spectrum was taken at room temperature in the region $500\text{--}2000\text{ cm}^{-1}$. The bands from silver nitrate are located at 732.8, 800.3, 833.1 and 1384.6 cm^{-1} . These values are in agreement with those reported in the literature (Miller and Wilkins 1952) (Table 1).

IR spectra from Brij 58, mesostructured SiO_2 :Brij 58 film (no silver) and mesostructured SiO_2 :Brij 58 film (with metallic silver NP's) were obtained. Table 2 contains the IR bands from Brij 58, which were identified in the positions at 551, 842, 957, 1061, 1105, 1241, 1342 and 1466 cm^{-1} . Similar bands were found in the spectra for films with and without metallic NP's. However, the bands located at $957\text{--}984\text{ cm}^{-1}$ from mesostructured films with and without silver NP's correspond to the stretching vibrations of silanol groups Si–OH (Martinez et al. 1998).

Figure 2 shows the IR spectra from the silica film with silver metallic NP's exposed to UV radiation for 6 h taken at room temperature in the region $400\text{--}4000\text{ cm}^{-1}$. Table 3 shows all the bands and the assignments.

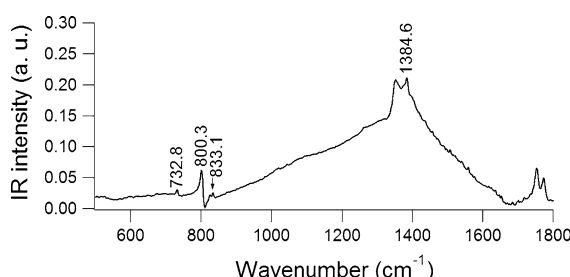


Fig. 1 Infrared spectrum of AgNO_3 powder

Table 1 IR frequencies (in cm^{-1}) from AgNO_3 powder

AgNO_3 Miller and Wilkins (1952)	$\text{AgNO}_3 + \text{KBr}$ Transmission	$\text{AgNO}_3 + \text{KBr}$ Diff. reflectance
733	732	731
803	800	802
835	833	834
1384	1385	1384

Table 2 IR frequencies (in cm^{-1}) from Brij 58, SiO_2 : Brij 58 and SiO_2 : Brij 58: AgNO_3 film

Surfactant Brij 58 v_{exp} (cm^{-1})	Mesostructured film with silver NP's v_{exp} (cm^{-1})	Mesostructured film, no silver v_{exp} (cm^{-1})
551	540	567
842	842	842
957	957.0	984.0
1061	1064	1061
1105	1109	1105
1241	—	1242
1342	1344	1342
1466	1466	1468

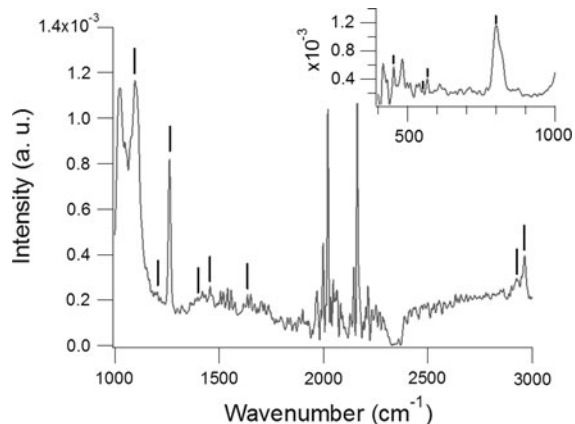


Fig. 2 IR spectra of the mesostructured SiO_2 :Brij 58 films with silver NP's after to UV exposition for 6 h

The band at 551.6 cm^{-1} corresponds to Brij 58 (Table 3). The bands at 453.3 , 567.1 , 798.5 , 1203.5 and 1635.6 cm^{-1} are IR spectroscopy of the silica (Jitianu et al. 2006; Jeon et al. 2003). These bands are due to bending Si–O–Si, Si–OH stretching, Si–O–Si asymmetric and symmetric stretching; respectively.

Table 3 IR frequencies and assignments

ν_{exp} (cm $^{-1}$)	Assignment	Reference
453.3	δ (Si–O–Si)	Jitianu et al. (2006)
551.6	Brij 58	Exp. meas.
567.1	ν (Si–OH)	Jeon et al. (2003)
731.0	NO_3^- ions	Jeon et al. (2003)
798.5	ν_s (Si–O–Si)	Miller and Wilkins (1952)
1097.5	C–O–C stretch.	Samarskaya and Dag (2001)
1203.5	ν_{as} (Si–O–Si)	Miller and Wilkins (1952)
1261.4	CH ₂ twisting	Samarskaya and Dag (2001)
1382.9	NO_3^- ions	Jeon et al. (2003)
1456.2	NO_3^- ions	Jeon et al. (2003)
1635.6	H–O–H def.	Jeon et al. (2003)
2925.4	ν_{as} (CH)(CH ₂)	Mondragon et al. (1995)
2964.5	ν_{as} (CH)(CH ₃)	Mondragon et al. (1995)

Exp. meas. experimental measurements

The band at 798.5 cm $^{-1}$ is attributed to the ring structure of the SiO tetrahedral (Jeon et al. 2003). The presence of the peak at 1261.4 cm $^{-1}$ is referred to the CH₂ twisting mode (Samarskaya and Dag 2001). The band at 1097.5 cm $^{-1}$ corresponds to C–O–C stretching. The band at 1635.6 cm $^{-1}$ is due to the H–O–H deformation which interacts through hydrogen bonds with silanol groups. The bands at 1382.9 and 1456.2 cm $^{-1}$ are attributed to NO₃ $^-$ ions (Jeon et al. 2003). All of these indicate the interaction of silver with the oxygen of ethylene oxide units of the surfactant molecules. The Ag $^+$ ions undergo complexation with the surfactant molecules, Ag $^+$ /Brij 58/NO₃ $^-$ (Samarskaya and Dag 2001).

Raman spectra

Raman spectra for Brij 58 powder and mesostructured film with silver NP's were obtained using 530.9 nm excitation. The spectra are shown in Fig. 3. The observed frequencies (in wavenumbers) are summarized in Table 4.

The bands at 798 and 1077 cm $^{-1}$ to Si–O–Si symmetric and asymmetric stretching modes, respectively, and the 966 cm $^{-1}$ peak to a Si–OH stretching vibration mode (Hu et al. 2007).

The IR frequencies (Table 3) are compared with those Raman frequencies (Table 4). The bands located at 1105, 1245 and 1484 cm $^{-1}$ can be attributed to the surfactant Bri58.

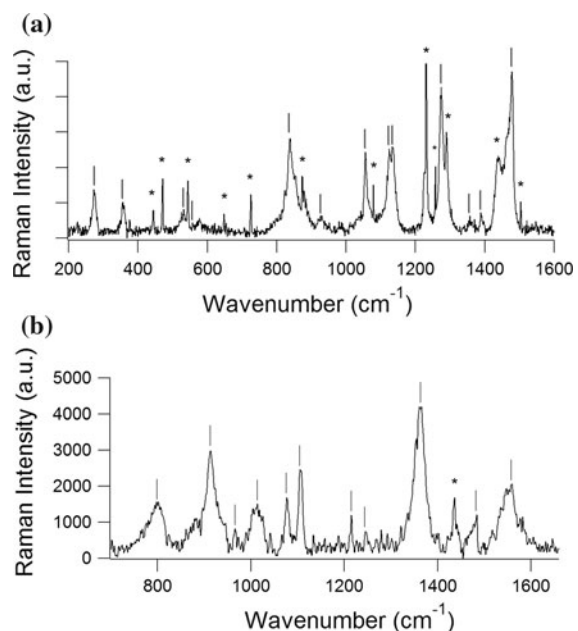


Fig. 3 Raman spectra of **a** Brij 58 powder and **b** mesostructured film with silver NP's, using 530.9 nm excitation

Table 4 Raman frequencies and intensities

Surfactant Brij 58	Mesostructured film with silver NP's
ν_{exp} (cm $^{-1}$)	ν_{exp} (cm $^{-1}$)
272.9	–
356.2	–
531.2	–
557.3	–
–	798
838.5	–
–	913
930.2	966
–	1014
1055.0	1077
–	1105
1124.0	–
1133.3	–
–	1215
1274.0	1245
1357.3	1365
1388.5	–
1478.1	1484
–	1558

X-ray diffraction

Figure 4 shows the XRD patterns at high angle of mesostructured (a) SiO_2 :Brij 58 film (grey solid line) and (b) SiO_2 :Brij 58 film with silver NP's (black solid line). The surfactant peaks were identified with an asterisk. Figure 4b reveals the presence of the silver oxide shell surrounding the metallic silver core by the diffraction peaks of silver oxide located at $2\theta = 26.95, 29.85, 32.25, 33.40$ and 44.50 . These peaks can be indexed as (110), (11-1), (120), (031) and (032), respectively, using the ASTM data card (#40-1054). For metallic silver, three diffraction peaks are located at $2\theta = 38.20, 64.60$ and 77.65 , and they were indexed as (111), (220) and (311), respectively, using ASTM data card (#01-1167). The intensity of the peaks from surfactant is more intense than those from silver oxide and silver NP's.

Initially, we established the acidic and reducing conditions for AgNO_3 salt in Brij58 surfactant and used it as a template for silica polymerization in the synthesis of uniformly distributed silver ions containing mesoporous silica matrix. After, the silver metallic NP's were produced during the UV exposition for 6 h of the films under air atmosphere in sol-gel silica films. These NP's can be oxidized in the pores of the silica gel due to (i) the interaction of the metallic NP's with oxygen causes oxidation on their surface and (ii) a light warming of the sample produced by the UV lamp which was very close to the film (3 cm). In this way the silver oxide phase was formed in a reducing environment.

Figure 5 shows the XRD pattern of mesostructured silica film with silver NP's. The peak at $2\theta = 1.77^\circ$, or a d -spacing of 49.9 \AA , corresponds to the (100)

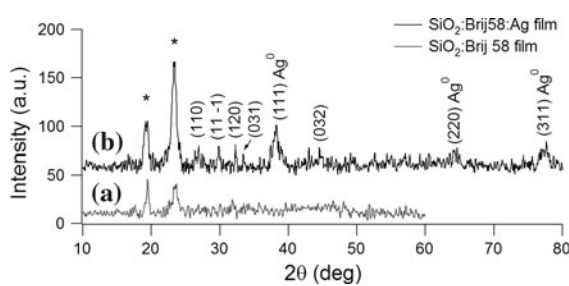


Fig. 4 XRD patterns at high angle of (a) SiO_2 :Brij 58 film (grey solid line), and (b) SiO_2 :Brij 58 film with silver metallic NP's (black solid line)

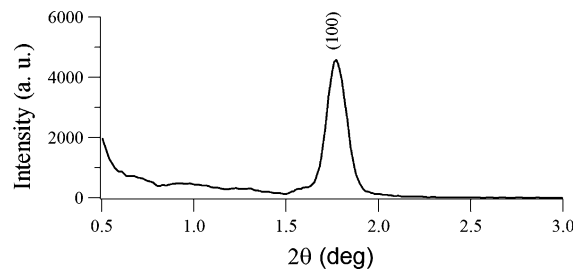


Fig. 5 XRD pattern of SiO_2 :Brij 58 film with silver NP's showing a hexagonal phase

peak revealing the formation of 2D-hexagonal phase in the SiO_2 host matrix.

Optical absorption spectra

The films were exposed to UV radiation for 6 h. Through this first method, silver metallic particles in the nanometre size range were produced in the mesostructured SiO_2 host matrix. The second possible reduction process of the AgNO_3 salt was induced by using of the non-ionic diblock copolymer (Brij 58) (Liz-Marzán and Lado-Touriño 1996). A colourless film was obtained when only silver ions were present in the matrix. On the other hand, the presence of the silver metallic NP's can be identified by the dark brown colour of the sol-gel films acquired after exposition to UV light for 6 h.

In addition to the colour change, the formation of these silver metallic NP's was followed by UV-Vis optical absorption spectroscopy. Figure 6 shows the optical absorption spectra taken at room temperature in the range of 300–900 nm. The absorption spectrum of the colourless SiO_2 :Brij 58 film does not exhibit any band (grey line). The spectrum of the black

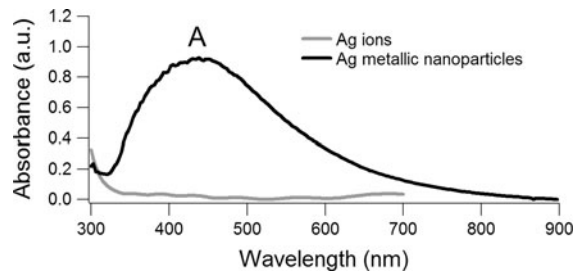


Fig. 6 Absorption spectra of the mesostructured SiO_2 :Brij 58 film with silver ions corresponding to a colourless silica film (grey solid line), and a mesostructured SiO_2 :Brij 58 film with silver metallic NP's (black solid line)

$\text{SiO}_2\text{-Brij}$ 58 film (black line) shows an absorption band A located at 440 nm. This spectrum shows a broad and asymmetric band suggesting the presence of silver metallic NP's of non-uniform size. For silver NP's under oxidizing atmosphere embedded in silica gels have been reported an absorption peak centred at 425 nm (Rentería-Tapia and García-Macedo 2005, 2006). A red shift was observed in our spectrum, it can be attributed to deformed silver particles covered with a silver oxide shell.

HRTEM measurements

A regular distribution of metallic NP's was observed. Figure 7a displays a TEM image showing small metallic silver NP's randomly oriented with spherical and prolate shapes. Figure 7b shows the HRTEM image of one silver nanoparticle. Its electron

d = 0.23 nm, which is consistent with (111) lattice of fcc Ag (Rentería-Tapia and García-Macedo 2008). According with these images, the optical properties observed in the absorption spectrum (Fig. 7) are due to metallic silver NP's. Figure 7c shows the HRTEM image of one silver oxide formed in these structures. The spacing between two crystal layers is $d = 0.322$ nm, which is consistent with the reflection (110) corresponding to silver oxide. Figure 7d exhibits the reflections for silver NP's, (202) and (220) with spacing of $d = 0.167$ nm and $d = 0.142$ nm, respectively. While, for silver oxide, the reflections (12-2) and (041) have spacing of $d = 0.219$ nm and $d = 0.213$ nm, respectively.

HRTEM images obtained with filtered energy of 10 eV, shown core–shell structures of metallic silver–

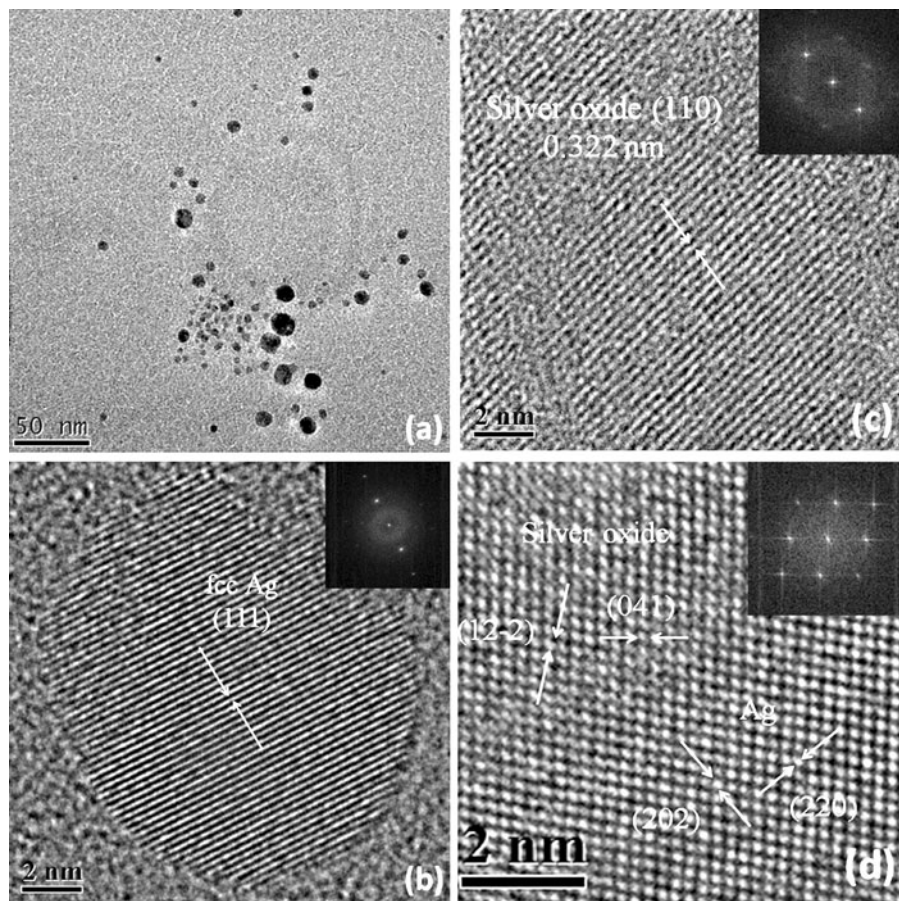


Fig. 7 Representative HRTEM micrographs of mesostructured $\text{SiO}_2\text{-Brij}$ 58 film with silver metallic NP's exposed to UV radiation for 6 h. **a** TEM image of the small metallic silver

NP's with spherical or prolate shapes. **b** HRTEM image of crystalline silver nanoparticle

silver oxide (Fig. 8). It is easy to observe that the dark shell corresponds to the silver oxide which is surrounding the silver metallic particle. In turn, a thin bright shell is covering the system metallic silver–silver oxide shell. This bright shell is related with the molecules of the surfactant Brij 58. In particular, these SiO_2 :Brij 58 films showed the SERS (Surface-enhanced Raman scattering) effect (García-Macedo et al. 2004). It is well known that the SERS is a process in which the Raman scattering cross-section of molecules absorbed onto the surfaces of metals such as silver, copper and gold is increased by as much as six orders of magnitude compared with the cross-section for normal Raman scattering. It means that the Raman signal from surfactant was increased when it covers the silver NP's.

The core–shell structures were stabilized by the surfactant shell obtaining a good particle size control and preventing the aggregation of the silver NP's. The Brij 58 allowed the control of small sizes and specific shapes (prolates and almost spherical) of the NP's. Therefore, the nature and concentration of this surfactant are crucial parameters to control the stability and optical properties of the particles. Finally, the block copolymer shell and silver oxide shell are very thin; it means that the first one did not allow that the second one expands too much. Therefore, the oxidation process of the silver NP's was inhibited.

From HRTEM micrographs, the corresponding size-distribution histograms were obtained (Fig. 9).

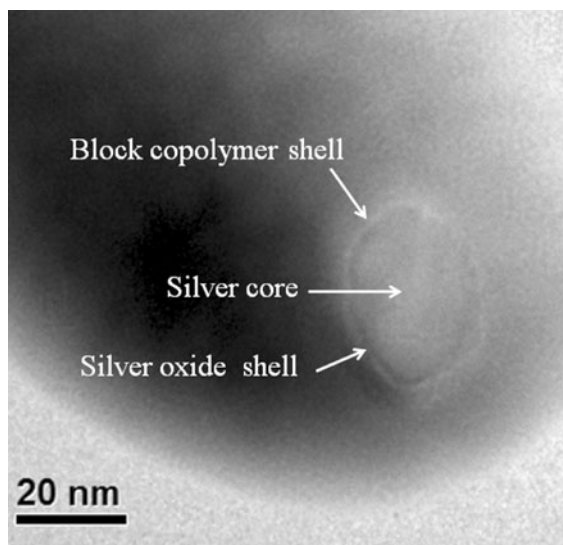


Fig. 8 HRTEM image of the resulting core–shell structure

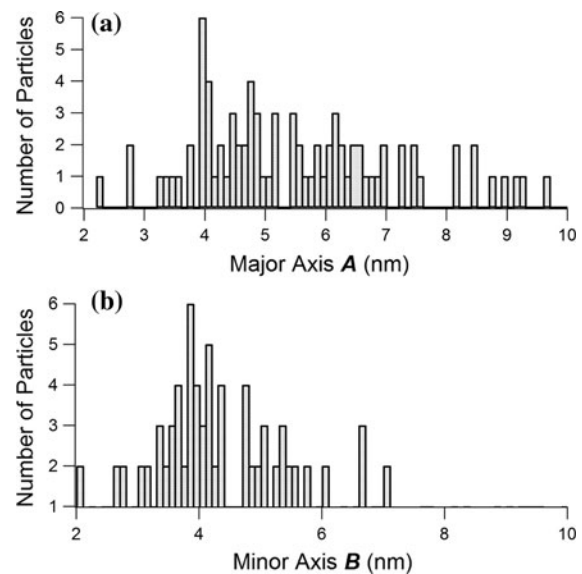


Fig. 9 Size-distribution histograms obtained by HRTEM analysis of silver NP's embedded in the SiO_2 :Brij 58 film

The distributions from the major axis A and minor length axis B of the metallic NP's are very broad. We obtained as average $A = 6.1 \pm 2.3$ nm (Fig. 9a), $B = 5.5 \pm 2.6$ nm (Fig. 9b), and the mean axial ratio AR was 0.80. The average size of the silver NP's was $2R < 20$ nm and therefore the Gans theory can be used to fit the optical absorption spectrum of the silver metallic silica film.

Rentería-Tapia and García-Macedo (2006) demonstrated that the Gans theory is adequate for sol–gel systems. They considered the case of the interactions between silver NP's and the dielectric medium by using two principal refractive indexes in their fits. One refractive index corresponds to NP's without silver oxide shell, and the other one index corresponds to the system silver core–silver oxide shell. Using this idea, the envelope corresponding to the calculated absorption spectrum can be obtained from adding the absorption bands of prolate NP's calculated with pairs of optical parameters: radii R_1 and R_2 , axial ratio Θ_1 and Θ_2 and two principal refractive indexes n_1 and n_2 to fit the experimental absorption spectrum (Fig. 6).

The experimental and calculated spectra of isolated silver NP's in mesostructured SiO_2 :Brij 58 films are shown in Fig. 10. In the fit done with the Gans theory for isolated silver particles, the dielectric constants $\varepsilon_1(\omega)$ and $\varepsilon_2(\omega)$ measured by Johnson and Christy (1972) were used, and it was considered

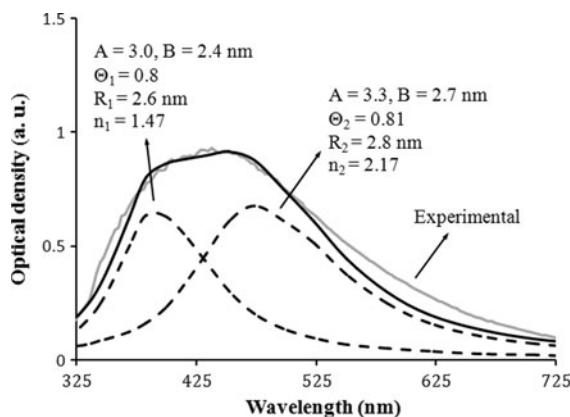


Fig. 10 Experimental absorption spectrum (*grey solid line*) from mesostructured SiO_2 :Brij 58 film with silver metallic NP's. Calculated absorption spectrum (*black solid line*) was obtained using our Gans model. The envelope is the result from the convolution of the component bands (*black dotted lines*) observed in the figure

$\omega_p = 1.38 \times 10^{16} \text{ s}^{-1}$ and $V_f = 1.4 \times 10^6 \text{ ms}^{-1}$ for silver (Rentería-Tapia and García-Macedo 2005). This fit was obtained by using the experimental data from size-distribution histograms of Fig. 9. The refractive index $n_1 = 1.47$ corresponding to the silica framework and the surfactant surrounding the NP's, which covers the silver NP's; and a high refractive index $n_2 = 2.17$ were used in Eqs. 2 and 3 to achieve this good fit. This last index is due to the silver oxide shell ($n = 2.5$) (Schmidt et al. 1996) and the surfactant shell formed around the silver NP's, and therefore the local refractive index grows with the oxidation process and determinates the maximum wavelength position of the surface plasmon resonance (Rentería-Tapia and García-Macedo 2005). Therefore, good fits were obtained using low and high refractive indexes ($n \geq 1.50$) in films exposed to UV radiation. The literature (Macdougall et al. 2002) reports for Brij 58 a refractive index equal to ~ 1.24 . This refractive index value is smaller than that from silver oxide shell $n_{\text{AgO}_2 \text{ shell}} > n_{\text{surfactant shell}}$. Then, the silver oxide shell has a more notable effect than the surfactant shell. These observed silver oxide shells surrounding the metallic particles suggest an important influence of the oxygen coming from the air atmosphere on the metallic NP's obtained in mesostructured SiO_2 :Brij 58 films. Consequently, the silver oxide shell-surfactant modifies the local surrounding medium of the metallic NP's and therefore

the optical properties of the films. This high refractive index of the dielectric medium produces the red shift of the peak of the optical absorption from NP's (Rentería-Tapia and García-Macedo 2006) observed in Fig. 6.

Conclusions

Stable optical properties were obtained from random-oriented silver prolate NP's embedded in mesostructured SiO_2 films prepared by the sol-gel method. Spherical/prolate silver NP's with sizes smaller than 12 nm were synthesised into a SiO_2 matrix through the reduction of silver ions by UV radiation. The use of the surfactant (Brij 58) allows controlling the size and shape of the silver NP's and their agglomeration was diminished.

Based on UV-Vis analysis and HRTEM images, it was possible to confirm that the silver NP's randomly dispersed were oxidized obtaining silver core–silver oxide shell. The second thin bright shell covering the metallic silver–silver oxide shell system corresponds to the surfactant. The observed red shift of the silver plasmon absorption band can be due to (i) the size and shape distribution of the NP's, (ii) the high local refractive index of the medium surrounding the NP's and (iii) the presence of free Ag^+ ions adsorbed onto the surface of the particles.

The physical characteristics of the system such as shape and size of the metallic NP's and the refractive index of silver oxide shell should be taken into account to obtain a good fit to the experimental optical absorption spectra. The contributions of silver core–silver oxide shell structures play an important role on the optical properties of the films.

Acknowledgments The authors acknowledge the financial supports of CONACYT 79781, Red NyN, PUNTA, DGAPA IN110808-3 and PAPIIT IN107510. We thank to M. in Sci. Manuel Aguilar-Franco (XRD), Luis Rendón (TEM and HRTEM) and Diego Quiterio (for preparation of the samples for TEM and HRTEM studies) for technical assistance.

References

- Alberius PC, Frindell KL, Hayward RC, Kramer EJ, Stucky GD, Chmelka BF (2002) General predictive syntheses of cubic, hexagonal, and lamellar silica and titania mesostructured thin films. *Chem Mater* 14:3284–3294

- Bohren CF, Huffman DR (1983) Absorption and scattering of light by small particles. Wiley, New York
- Caseri WR (2006) Nanocomposites of polymers and inorganic particles: preparation, structure and properties. *Mater Sci Technol* 22:807–817
- Compagnini G, D'Urso L, Puglisi O (2002) Structure and properties of silver NP's dispersed in SiO_2 thin films obtained by in situ self-reduction. *Mater Sci Eng C* 19:295–298
- García-Macedo JA, Valverde G, Lockard J, Zink JI (2004) SERS on mesostructured thin films with silver NP's. *Proc SPIE*. doi: [10.1117/12.529756](https://doi.org/10.1117/12.529756)
- Hu J, Lee W, Cai W, Tong L, Zeng H (2007) Evolution of the optical spectra of an Ag/mesoporous SiO_2 nanostructure heat-treated in air and H_2 atmospheres. *Nanotechnology* 18:185710
- Jeon H-J, Yi S-C, Oh S-G (2003) Preparation and antibacterial effects of Ag- SiO_2 thin films by sol-gel method. *Biomaterials* 24:4921–4928
- Jitianu A, Raileanu M, Crisan M, Predoi D, Jitianu M, Stanciu L, Zaharescu M (2006) Fe_3O_4 - SiO_2 nanocomposites obtained via alkoxide and colloidal route. *J Sol-Gel Sci Technol* 40:317–323
- Johnson PB, Christy RW (1972) Optical constants of the noble metals. *Phys Rev B* 6:4370–4379
- Kozuka H (1997) Metal NP's in gel-derived oxide coating films: control and application of surface plasma resonance. *Proc SPIE*. doi: [10.1117/12.279166](https://doi.org/10.1117/12.279166)
- Link S, Mohamed MB, El-Sayed MA (1999) Simulation of the optical absorption spectra of gold nanorods as a function of their aspect ratio and the effect of the medium dielectric constant. *J Phys Chem B* 103:3073–3077
- Liz-Marzáñ LM, Lado-Touriño I (1996) Reduction and stabilization of silver NP's in ethanol by nonionic surfactants. *Langmuir* 12:3585–3589
- Macdougall JE, Heier KR, Weigel SJ (2002) US Patent No. 20020102396, <http://www.patentstorm.us/patents/6365266-description.html>
- Martinez JR, Ruiz F, Vorobiev YV, Perez-Robles F, Gonzalez-Hernandez J (1998) Infrared spectroscopy analysis of the local atomic structure in silica prepared by sol-gel. *J Chem Phys* 109:7511–7514
- Masumoto Y, Kawamura T (1993) Biexciton lasing in CuCl quantum dots. *App Phys Lett* 62:225–227
- Miller FA, Wilkins CH (1952) Infrared spectra and characteristic frequencies of inorganic ions. *Anal Chem* 24:1253–1294
- Mondragon MA, Castaño VM, García-Macedo J, Téllez CA (1995) Vibrational analysis of $\text{Si}(\text{OC}_2\text{H}_5)_4$ and spectroscopic studies on the formation of glasses via silica gels. *Vib Spectrosc* 9:293–304
- Naoi K, Ohko Y, Tatsuma T (2004) TiO_2 films loaded with silver NP's: control of multicolor photochromic behavior. *J Am Chem Soc* 126:3664–3668
- Nishida F, McKiernan JM, Dunn B, Zink JI, Brinker CJ, Hurd AJ (1995) In situ fluorescence probing of the chemical changes during sol-gel thin film formation. *J Am Ceram Soc* 78:1640–1648
- Pérez-Juste J, Pastoriza-Santos I, Liz-Marzáñ LM, Mulvaney P (2005) Gold nanorods: synthesis, characterization and applications. *Coord Chem Rev* 249:1870–1901
- Rentería-Tapia VM, García-Macedo JA (2005) Modeling of optical absorption of silver prolate NP's embedded in sol-gel glasses. *Mater Chem Phys* 91:88–93
- Rentería-Tapia VM, García-Macedo JA (2006) Influence of the local dielectric constant on modelling the optical absorption of silver NP's in silica gels colloids. *Colloids Surf A* 278:1–9
- Rentería-Tapia VM, García-Macedo JA (2008) Influence of oxygen on the optical properties of silver nanoparticles. *J Nanosci Nanotechnol* 8:6545–6550
- Samarskaya O, Dag Ö (2001) Silver nitrate/oligo(ethylene oxide) surfactant/mesoporous silica nanocomposite films and monoliths. *J Colloid Interf Sci* 238:203–207
- Schmidt AA, Offermann J, Anton R (1996) The role of neutral oxygen radicals in the oxidation of Ag films. *Thin Solid Films* 281–282:105–107
- Smarsly B, Polarz S, Antonietti M (2001) Preparation of porous silica materials via sol-gel nanocasting of nonionic-surfactants: a mechanistic study on the self-aggregation of amphiphiles for the precise prediction of the mesopore-size. *J Phys Chem B* 105:10473–11048
- Sun Y, Mayers B, Xia Y (2003) Transformation of silver nanospheres into nanobelts and triangular nanoplates through a thermal process. *Nano Lett* 3:675–679
- Weiping C, Ming T, Lide Z (1996) Characterization and the optical switching phenomenon of porous silica dispersed with silver nano-particles within its pores. *J Phys* 8:L591–L596
- Winkler H, Birkner A, Hagen V, Wolf I, Schmeichel R, Seggern H, Fischer RA (1999) Quantum-confined gallium nitride in MCM-41. *Adv Mater* 11:1444–1448
- Xu H, Käll M (2002) Modeling the optical response of nanoparticle-based surface plasmon resonance sensors. *Sens Actuators B* 87:244–249